JOURNAL OF MATERIALS SCIENCE 28 (1993) 6091–6095

Crystallization studies on amorphous Al–Y–Ni and Al–Y–Cu alloys

A. GOYAL, B.S. MURTY, S. RANGANATHAN
Department of Metallurgy, Indian Institute of Science, Bangalore 560 012, India

$Al_{83}Y_{10}Ni_7$, $Al_{80}Y_{10}Ni_{10}$ and $Al_{80}Y_{10}Cu_{10}$ alloys were studied by the rapid solidification processing route. The glass-forming ability was found to decrease in the order of alloys mentioned above. Differential scanning calorimetry (DSC) of these amorphous alloys showed that the amorphous phase in Al–Y–Ni alloys has a higher thermal stability when compared to that in Al–Y–Cu alloys. A four-stage crystallization sequence could be identified for the Al–Y–Ni amorphous alloys. Even though the $Al_{80}Y_{10}Cu_{10}$ alloy showed four exothermic peaks in the DSC study, a definite crystallization sequence could not be arrived at due to the coexistence of many crystalline phases along with the amorphous phase in the melt-spun condition.

1. Introduction

Since the pioneering work of a group of investigators led by Duwez [1] which reported the first metallic glass in an Au–20 at % Si alloy by melt-quenching, metallic glasses synthesized by melt-quenching, more widely known as rapid solidification processing, have been of interest to materials scientists. The special properties of these metallic glasses, such as high strength, high corrosion resistance, high electrical resistivity, low eddy current and magnetic hysteresis losses have made them not only scientifically but also commercially important.

Since the 1960s there have been attempts to produce Al-based metallic glasses by rapid solidification processing with the expectation of high specific strength due to the low density of these alloys. Studies on Al-based metallic glasses have been recently reviewed by Inoue *et al.* [2] with emphasis on the extensive Japanese contributions to the field. The initial experiments on binary Al alloys such as Al–Si [3], Al–Ge [4], Al–Cu [5], Al–Ni [6], Al–Cr [7] and Al–Pd [8] by the gun-quenching technique could yield only coexistence of the amorphous phase with crystalline phases. Later, it was found that the glass-forming ability of Al-based alloys improved with the addition of ternary elements. The formation of single-phase amorphous Al-based alloy by rapid solidification processing was first reported by Inoue *et al.* [9] in Al–Fe–B and Al–Co–B systems. However, these alloys were found to be very brittle. It was only in 1987 [10] that a ductile amorphous phase was synthesized in Al–Ni–Si and Al–Ni–Ge alloys which contained more than 80 at% Al.

Al–Y–Ni and Al–Y–Cu amorphous alloys fall under the Al–lanthanide metal–transition metal systems which have been widely studied by Inoue *et al.* [11, 12] for the glass-forming composition ranges. However, little work has been done on the thermal stability and crystallization sequence of Al-based metallic glasses. Inoue *et al.* [11–13] have studied the composition dependence of crystallization temperature. Very recently, Kwong *et al.* [14] and Cao *et al.* [15] have studied $Al_{85}Y_{10}Ni_5$ and $Al_{88.5}Y_{6.5}Ni_5$, respectively, with emphasis on the crystallization sequence of the amorphous phase. The present paper reports a study of the crystallization behaviour of amorphous $Al_{83}Y_{10}Ni_7$, $Al_{80}Y_{10}Ni_{10}$ and $Al_{80}Y_{10}Cu_{10}$ alloys.

2. Experimental procedure

The $Al_{83}Y_{10}Ni_7$, $Al_{80}Y_{10}Ni_{10}$ and $Al_{80}Y_{10}Cu_{10}$ alloys were made by induction-melting of high-purity metals under an argon atmosphere. The melt-spinning experiments were carried out on a single Cu roller at linear wheel velocities of 31, 41 and 47 m s^{-1}. The crystallization studies of the melt-spun alloys were carried out in a differential scanning calorimeter (DSC) (Perkin-Elmer DSC-2C) in the temperature range of 320–999.9 K with different heating rates of 10, 20, 40 and 80 K min^{-1}. After heating the alloy to the required temperature in the DSC, the sample was cooled rapidly in the DSC at a rate of 320 K min^{-1} to retain the transformation products. The as-cast, melt-spun and DSC heat-treated samples were characterized in a Huber–Guinier X-ray diffractometer (XRD) with CuK_α radiation ($\lambda = 0.154\,05$ nm). Transmission electron microscopy (TEM) was performed using a Jeol 2000 FX II operating at 200 kV.

3. Results

3.1. $Al_{83}Y_{10}Ni_7$

Fig. 1a shows the XRD pattern of the as-cast $Al_{83}Y_{10}Ni_7$ alloy. The alloy in the as-cast condition showed only α-Al and Al_3Y phases with α-Al peaks being the most intense, indicating the presence of higher volume fraction of α-Al. The figure also shows

0022–2461 © *1993 Chapman & Hall*

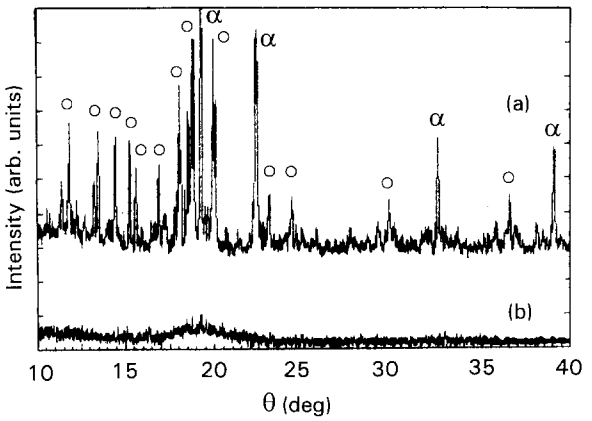

Figure 1 XRD patterns of $Al_{83}Y_{10}Ni_7$ alloy in (a) as-cast and (b) melt-spun (31 m s^{-1}) conditions; (α) α-Al, (○) Al_3Y.

the XRD pattern of the alloy melt-spun at 31 m s^{-1} (Fig.1b) which shows an amorphous broad peak. The fact that the melt-spun sample was completely amorphous was confirmed by TEM. Fig. 2 gives the selected-area diffraction pattern of this sample, showing a diffuse halo indicative of the amorphous nature of the alloy. The melt-spun alloy had good bend ductility which allowed the foils to be bent up to 180° without fracture.

The melt-spun alloy was studied by DSC and Fig. 3a shows the DSC trace of the alloy at a heating rate of 40 K min^{-1}. Four exothermic peaks and an endothermic peak were observed in the temperature range of 320–950 K. The crystallization peak for the amorphous phase was observed at 576 K, followed by three exothermic peaks corresponding to the formation of equilibrium phases at 612, 655 and 748 K. Finally, the alloy melted at 926 K. The enthalpies of crystallization and other transformations were calculated from the area under the peaks and are tabulated in Table I.

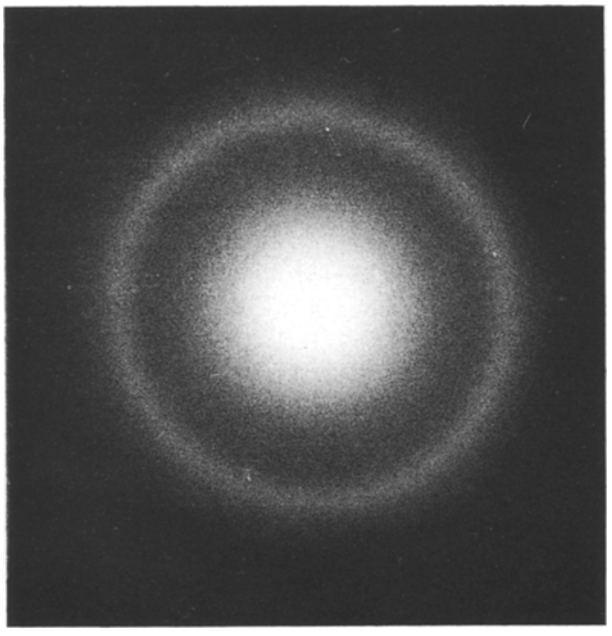

Figure 2 Selected-area electron diffraction pattern of $Al_{83}Y_{10}Ni_7$ alloy melt-spun at a wheel speed of 31 m s^{-1}.

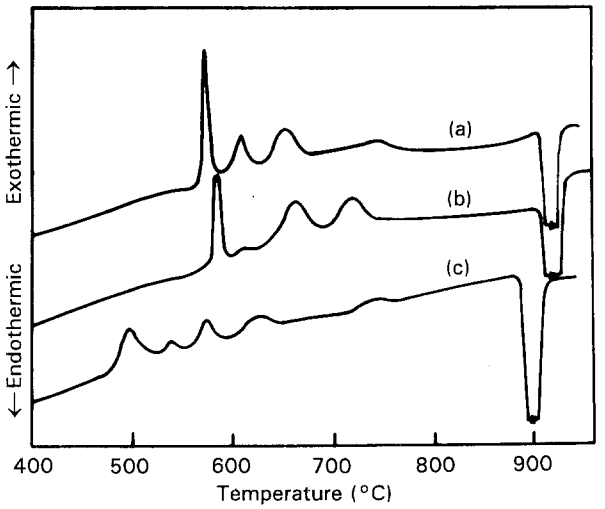

Figure 3 DSC trace of (a) $Al_{83}Y_{10}Ni_7$, (b) $Al_{80}Y_{10}Ni_{10}$ and (c) $Al_{80}Y_{10}Cu_{10}$ at the heating rate of 40 K min^{-1}.

TABLE I DSC results for $Al_{83}Y_{10}Ni_7$ alloy at the heating rate of 40 K min^{-1}

	Transformation temperature (K)	Enthalpy of transformation (kJ mol^{-1})	Activation energy (kJ mol^{-1})
Exotherm 1	576	1.65	328
Exotherm 2	612	0.49	244
Exotherm 3	655	0.99	201
Exotherm 4	748	0.19	250

The indium melting peak was taken as the reference for these calculations. The enthalpy of crystallization (1.65 kJ mol^{-1}) was found to be much more than that of other transformations. The activation energy for transformations was calculated from the variation of transformation temperature with heating rate in DSC using the Kissinger–Boswell method [16, 17] and the results are presented in Table I. Similar to the enthalpy of crystallization, the activation energy for crystallization was also found to be more than that of the other transformations leading to equilibrium phases.

In order to determine the products of transformations the melt-spun foils of the alloy were heated in the DSC at 40 K min^{-1} and quenched after each peak at the rate of 320 K min^{-1}. These quenched samples were characterized by XRD and results are shown in Fig. 4. The phases observed in the DSC-quenched samples, along with the as-cast and melt-spun ones, are shown in Table II. The alloy after the crystallization peak showed α-Al along with amorphous phase. The sample quenched after the second exotherm showed additional XRD peaks which could be identified as Al_3Y and the amorphous broad peak disappeared. The phases present after the third exotherm were α-Al, Al_3Y and AlYNi. The ternary AlYNi phase disappeared after the fourth exotherm and the equilibrium Al_3Ni was formed.

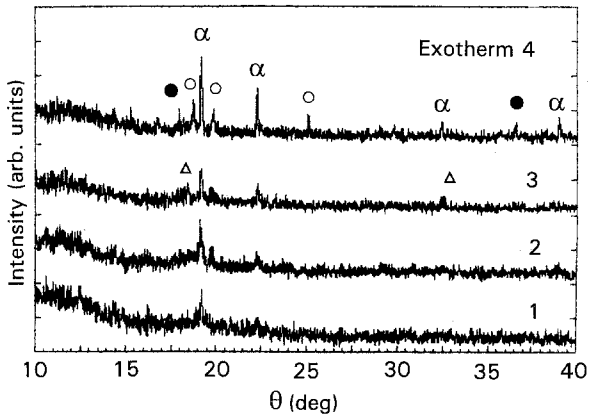

Figure 4 XRD patterns of $Al_{83}Y_{10}Ni_7$ alloy quenched in DSC from the different exotherms; (α) α-Al, (○) Al_3Y, (●) Al_3Ni, (△) AlYNi.

TABLE II Phases present in $Al_{83}Y_{10}Ni_7$ alloy under different processing conditions

Condition	Phases
As-cast	α-Al and Al_3Y
Melt-spun, 31 m s^{-1}	Amorphous
Exotherm 1	α-Al and amorphous
Exotherm 2	α-Al and Al_3Y
Exotherm 3	α-Al, Al_3Y and AlYNi
Exotherm 4	α-Al, Al_3Y and Al_3Ni

3.2. $Al_{80}Y_{10}Ni_{10}$

XRD analysis of the as-cast alloy revealed the presence of α-Al and Al_3Y (Fig. 5a) similar to the $Al_{83}Y_{10}Ni_7$ alloy (Fig.1a). Melt-spinning of the alloy at a wheel speed of 31 m s^{-1} did not result in amorphization and the sample showed the presence of only α-Al (Fig. 5b). Increasing the wheel speed to 41 m s^{-1} resulted in glass formation (Fig. 5c) which was confirmed by TEM study.

The DSC study showed four exothermic peaks at 586, 610, 665 and 722 K and an endotherm at 927 K corresponding to melting at the heating rate of 40 K min^{-1} as shown in Fig. 3b. The enthalpy and activation energy for transformation calculated for the four exotherms are presented in Table III. The phases

TABLE III DSC results for $Al_{80}Y_{10}Ni_{10}$ alloy at the heating rate of 40 K min^{-1}

	Transformation temperature (K)	Enthalpy of transformation (kJ mol^{-1})	Activation energy (kJ mol^{-1})
Exotherm 1	586	2.04	294
Exotherm 2	610	0.07	246
Exotherm 3	665	0.92	204
Exotherm 4	742	0.66	217

observed from the XRD patterns of the DSC-quenched samples after each exotherm (Fig. 6) are shown in Table IV, and were the same as those observed in the case of $Al_{83}Y_{10}Ni_7$.

3.3. $Al_{80}Y_{10}Cu_{10}$

The XRD patterns of the as-cast $Al_{80}Y_{10}Cu_{10}$ alloy (Fig. 7a) showed a large number of peaks. In contrast to the Al–Y–Ni alloys, in this alloy α-Al peaks were not the most intense. The phase corresponding to the most intense peaks could be identified as tetragonal Al_4Y which was not observed in the Al–Y–Ni alloys. Apart from these two phases, the as-cast alloy also showed Al_3Y and Al_2Cu. Melt-spinning of this alloy did not result in complete amorphization. Even at the wheel speed of 47 m s^{-1}, which was the maximum achievable in the present set-up, crystalline phases coexisted with amorphous phase (Fig. 7b). This is supported by the selected-area electron diffraction pattern of the melt-spun alloy as shown in Fig. 8. The XRD pattern of the melt-spun alloy showed α-Al, Al_4Y, Al_3Y and ternary AlYCu phases along with the amorphous phase.

The DSC study of the alloy showed five exothermic peaks at 499, 540, 576, 632 and 742 K and an endothermic melting peak at 901 K at the heating rate of 40 K min^{-1}. The enthalpy and activation energies for transformations were calculated for these exotherms and are presented in Table V. The XRD patterns of the DSC quenched samples from each exotherm are shown in Fig. 9. The samples corresponding to the first two exotherms showed the same

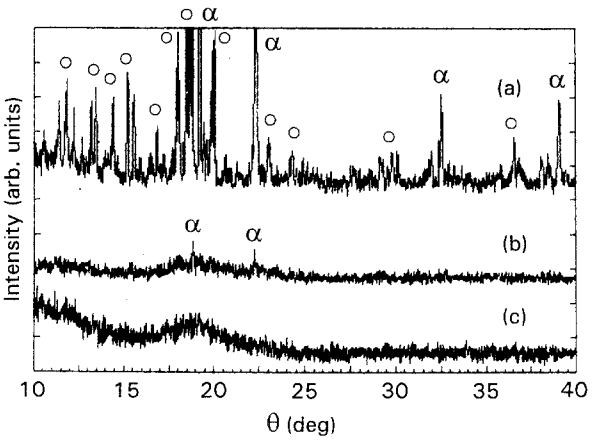

Figure 5 XRD patterns of $Al_{80}Y_{10}Ni_{10}$ alloy (a) as-cast, (b) melt-spun at 31 m s^{-1} and (c) melt-spun at 41 m s^{-1}, (α) α-Al, (○) Al_3Y.

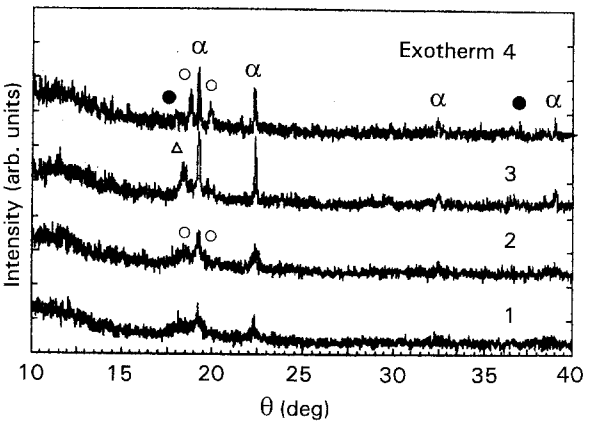

Figure 6 XRD patterns of $Al_{80}Y_{10}Ni_{10}$ alloy quenched in DSC from the different exotherms; (α) α-Al, (○), Al_3Y, (●) Al_3Ni, (△) AlYNi.

TABLE IV Phases present in $Al_{80}Y_{10}Ni_{10}$ alloy under different processing conditions

Condition	Phases
As-cast	α-Al and Al_3Y
Melt-spun, 31 m s^{-1}	α-Al
Melt-spun, 41 m s^{-1}	Amorphous
Exotherm 1	α-Al and amorphous
Exotherm 2	α-Al and Al_3Y
Exotherm 3	α-Al, Al_3Y and AlYNi
Exotherm 4	α-Al, Al_3Y and Al_3Ni

TABLE V DSC results for $Al_{80}Y_{10}Cu_{10}$ alloy at the heating rate of 40 K min^{-1}

	Transformation temperature (K)	Enthalpy of transformation (kJ mol^{-1})	Activation energy (kJ mol^{-1})
Exotherm 1	499	0.83	146
Exotherm 2	540	0.12	234
Exotherm 3	576	0.39	186
Exotherm 4	632	0.46	193
Exotherm 5	742	0.25	179

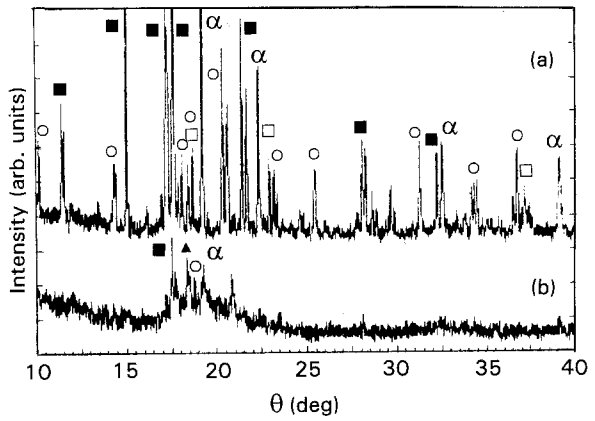

Figure 7 XRD patterns of $Al_{80}Y_{10}Cu_{10}$ alloy in (a) as-cast and (b) melt-spun (47 m s^{-1}) conditions; (α) α-Al, (○) Al_3Y, (■) Al_4Y, (□) Al_2Cu, (▲) AlYCu.

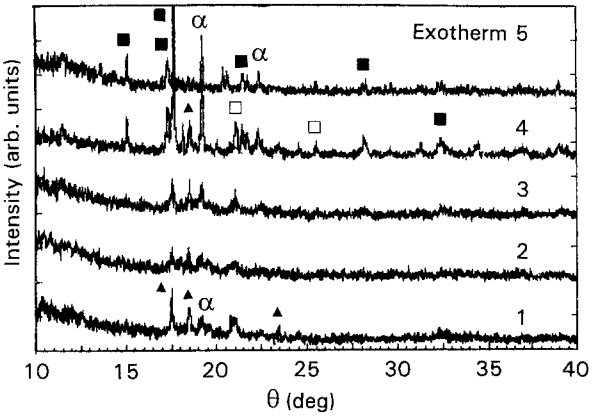

Figure 9 XRD patterns of $Al_{80}Y_{10}Cu_{10}$ alloy quenched in DSC from the different exotherms; (α), α-Al, (■) Al_4Y, (□) Al_2Cu, (▲) AlYCu.

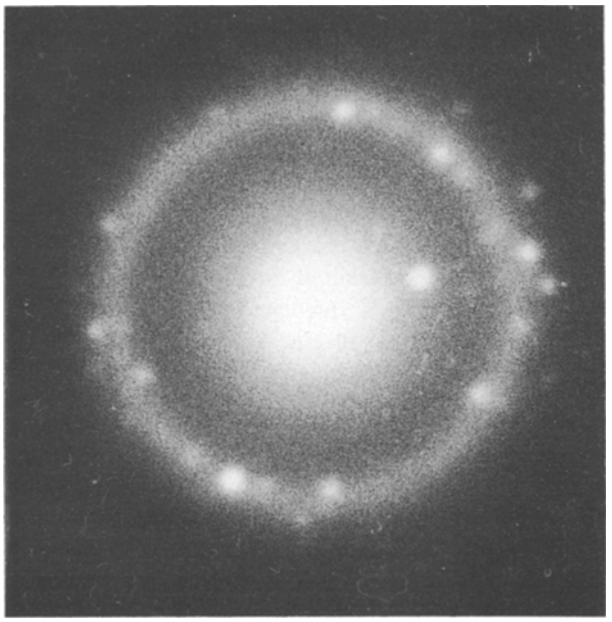

Figure 8 Selected-area electron diffraction pattern of $Al_{80}Y_{10}Cu_{10}$ alloy melt-spun at a wheel speed of 47 m s^{-1}.

phases, α-Al and AlYCu. The third exotherm resulted in the formation of Al_2Cu. The fourth exotherm showed Al_4Y in addition to the above three phases. Finally, after the fifth exotherm, Al_2Cu and AlYCu disappeared leaving only α-Al and Al_4Y as shown in Table VI.

TABLE VI Phases present in $Al_{80}Y_{10}Cu_{10}$ alloy under different processing conditions

Condition	Phases
As-cast	α-Al, Al_4Y, Al_3Y and Al_2Cu
Melt-spun, 47 m s^{-1}	α-Al, Al_4Y, Al_3Y, AlYCu and amorphous
Exotherm 1	α-Al and AlYCu
Exotherm 2	α-Al and AlYCu
Exotherm 3	α-Al, AlYCu and Al_2Cu
Exotherm 4	α-Al, Al_4Y, AlYCu and Al_2Cu
Exotherm 5	α-Al and Al_4Y

4. Discussion

An important observation in the present study was that the glass-forming ability of the three alloys was different. The $Al_{83}Y_{10}Ni_7$ alloy was the easiest glass-former while the $Al_{80}Y_{10}Cu_{10}$ alloy was the most difficult glass-former, with the $Al_{80}Y_{10}Ni_{10}$ alloy falling midway. Similar observations have been reported earlier by Inoue *et al.* [11] with respect to the glass-forming composition ranges (GFRs), showing that the GFR is much narrower for the Al–Y–Cu system when compared to the Al–Y–Ni system. The thermal stability of Al–Y–Ni amorphous alloys was found to be much better than that of the Al–Y–Cu amorphous alloy in the present investigation. The crystallization temperature of the Al–Y–Ni amorphous phase was about 100 K higher than that of Al–Y–Cu. The crystallization temperature in the case

of all these alloys was in close agreement with that reported earlier [11] for the same compositions. However, Inoue *et al.* [11] did not report the other exotherms. Cao *et al.* [15] observed four exotherms in a crystallization study of the $Al_{88.5}Y_{6.5}Ni_5$ alloy. The crystallization peak temperature reported by them was 469 K, which was about 100 K less than that observed in the present study for Al–Y–Ni alloys. The enthalpy of crystallization observed in the present study for the Al–Y–Ni alloys ($\sim 2\,kJ\,mol^{-1}$) is less than that reported by Inoue *et al.* [13] ($\sim 3\,kJ\,mol^{-1}$).

Kwong *et al.* [14] observed a different number of stages of crystallization at different heating rates in differential thermal analysis in the range of 1–20 K min^{-1} for the $Al_{85}Y_{10}Ni_5$ alloy. The present results do not support this. In the range of 10–80 K min^{-1}, all three alloys showed the same number of crystallization stages at all heating rates, but the enthalpy of transformation was found to be a function of heating rate in all cases.

Both the Al–Y–Ni alloys were found to behave similarly in all aspects except that the glass-forming ability of $Al_{83}Y_{10}Ni_7$ was found to be better than that of $Al_{80}Y_{10}Ni_{10}$. For both alloys a four-stage crystallization process could be conceived, based on the XRD results for the DSC-quenched samples for each exotherm. In the first stage of crystallization supersaturated α-Al precipitates by a primary crystallization process. In the second stage the remaining amorphous phase transforms eutectically into α-Al and Al_3Y. The third stage could be thought of as the solid-state precipitation of ternary AlYNi phase from the supersaturated α-Al. The ternary AlYNi phase, being metastable, transforms into Al_3Y and Al_3Ni in the fourth stage of crystallization, thus yielding equilibrium phases. The reactions at each exotherm can be put down as

Exotherm 1: amorphous phase → supersaturated α-Al

Exotherm 2: amorphous phase → α-Al + Al_3Y

Exotherm 3: supersaturated α-Al → α-Al + AlYNi

Exotherm 4: AlYNi → Al_3Ni + Al_3Y

A similar crystallization sequence has been proposed by Cao *et al.* [15] for the $Al_{88.5}Y_{6.5}Ni_5$ alloy, based on XRD results for the samples obtained after each exotherm in their differential thermal analysis. In the case of Al–Y–Cu alloy similar conclusions could not be reached, as the melt-spun alloy contained many crystalline phases along with the amorphous phase. The samples obtained from the first and second exotherms showed the same phases, namely, α-Al and AlYCu, which could be due to a lesser amount of transformation products of the second exotherm which could not be detected by the XRD.

5. Conclusions

1. The glass-forming ability of $Al_{83}Y_{10}Ni_7$ was the best among the three alloys studied. $Al_{80}Y_{10}Cu_{10}$ could not be completely amorphized in the present study, which indicates its poor glass-forming ability.

2. The thermal stability of Al–Y–Ni glasses was found to be much higher than that of the Al–Y–Cu glass.

3. A four-stage crystallization sequence was identified in the case of Al–Y–Ni alloys.

4. Even though five exotherms were observed in the case of Al–Y–Cu alloy a clear-cut picture of the crystallization process could not be arrived at, due to the large number of crystalline phases present in the melt-spun condition itself.

Acknowledgements

The authors are thankful to Professor K. Chattopadhyay, Professor D. H. Sastry and Mr. R. Goswami for useful discussions. The financial support of the Materials and Processes Panel of the Aeronautical Research and Development Board is gratefully acknowledged.

References

1. W. KLEMENT, R. H. WILLENS and P. DUWEZ, *Nature* **187** (1960) 869.
2. A. INOUE, K. OHTERA and T. MASUMOTO, *Sci. Rep. Res. Inst. Tohoku Univ.* **A-35** (1990) 115.
3. P. PREDECKI, B. C. GIESSEN and N. J. GRANT, *Trans. Met. Soc. AIME* **233** (1965) 1438.
4. P. RAMACHANDRA RAO, M. LARIDJANI and R. W. CAHN, *Z. Metallkde* **63** (1972) 43.
5. H. A. DAVIES and J. B. HULL, *Scripta Metall.* **6** (1972) 241.
6. K. CHATTOPADHYAY, P. RAMACHANDRA RAO, S. LELE and T. R. ANANTHARAMAN, in Proceedings of 2nd International Conference on Rapidly Quenched Metals, Cambridge, Massachusetts, edited by N. J. Grant and B. C. Giessen (MIT Press, 1976) p. 157.
7. P. FURRER and H. WARLIMONT, *Mater. Sci. Engng* **28** (1977) 127.
8. G. V. S. SASTRY, C. SURYANARAYANA, O. N. SRIVASTAVA and H. A. DAVIES, *Trans. Indian Inst. Met.* **31** (1978) 292.
9. A. INOUE, A. KITAMURA and T. MASUMOTO, *J. Mater. Sci.* **16** (1981) 1895.
10. A. INOUE, M. YAMAMOTO, H. M. KIMURA and T. MASUMOTO, *J. Mater. Sci. Lett.* **6** (1987) 194.
11. A. INOUE, K. OHTERA, A. P. TSAI and T. MASUMOTO, *Jpn. J. Appl. Phys.* **27** (1988) L280.
12. A. INOUE, K. OHTERA and T. MASUMOTO, *ibid.* **27** (1988) L1796.
13. A. INOUE, K. OHTERA, A. P. TSAI and T. MASUMOTO, *ibid* **27** (1988) L479.
14. V. KWONG, Y. C. KOO, S. J. THORPE and K. T. AUST, *Acta Metall.* **39** (1991) 1563.
15. B. CAO, S. LI and D. YI, *J. Less-Common Metals* **171** (1991) 1.
16. H. E. KISSINGER, *Anal. Chem.* **29** (1957) 1702.
17. P. G. BOSWELL, *J. Therm. Anal.* **18** (1980) 353.

Received 6 April 1992
and accepted 27 April 1993